

## The Influence of Porosity Value and Mode on Soft Polymer Materials Behaviour

D. Zeleniakienė\*, T. Kleveckas, J. Liukaitis, E. Fataraitė

Department of Design and Technologies, Kaunas University of Technology, Studentų 56, LT-3031 Kaunas, Lithuania

Received 09 October 2002; accepted 25 May 2003

The influence of soft polymer materials porosity size and mode on stress, deformability and size of deformation forces in model system have been investigated by computational finite element method and experimental method of photoelasticity. Plane models differ from each other in pores size and its distribution mode. To the ends of all of them deformation of constant value were added. It was obtained that in the case of small and rare pores the highest stress concentration zones appear compare to those of non-porous material. The evenly distributed of the same diameter pores with wide interpores zones increase stress concentration, also. The porosity mode influences the stress state only in the case of high material porosity: the high material porosity ( $\gamma > 0.5$ ) and the absence of large interpores zones decrease stress concentration and, in some cases, can be lower than those in nonporous material. Good correlation between experimental and calculated results was obtained.

*Keywords:* soft polymer material, porosity, stress state, stress concentration factor, finite element method, method of photoelasticity.

### INTRODUCTION\*

Microstructural modification of materials appears to be a promising route to change their mechanical properties during application. The prediction of effective properties of heterogeneous systems such as porous media or so-called porous composites, which exhibit a complex macrostructure, is of considerable interest [1]. These materials are characterised by the good technological and exploitation properties, they are softer and less in weight, compare to those nonporous.

These materials usually are applied in the constructions or as individual elements, which work under the creep conditions. As a rule they are used in buffers and are involved to work in various conditions for constant amplitude oscillations. Such elements work under constant value of impact loading, flexing, tensile conditions, for which large geometry and volume changes are characteristic. That causes high stresses and regions of its concentrations [2–4]. As a result is failure initiation and further fracture of element, which fracture periodically due to fatigue [5]. So, it is of great importance to know, which of factors is main reason for failure initiation, i.e. results on the creation of the high stressed regions during external loading.

The mechanical properties of porous materials at the macroscopic level are highly governed by their microstructure, which is characterized by the mechanical behaviour, geometrical arrangement, size and shape of pores presented in microstructure. The optimisation of these macroscopic mechanical properties can be achieved by the carefully adaptation of the microstructure.

The development of such materials is generally done empirically, that is, a large number of samples with different microstructures are fabricated and tested, until specific requirements on the mechanical behaviour of these materials are fulfilled. These trial and error methods are

usually time consuming and expensive. The more fundamental studies are needed for a better understanding of the deformation behaviour of these advanced materials. Relations between the microstructural phenomena and the macroscopic deformation behaviour are indispensable when predicting macroscopic properties from the microstructure of the material.

There are many results of research investigations [2, 6–10], in which influence of material porosity, cavity size, amount and distribution mode on the strength, thermo, filtering and other properties have been investigated. But the results related to investigation of soft polymer materials behaviour are limited. The main difference between solid and soft polymers is that for last the one high deformability at low stress values is characteristic. Meanwhile fracture of solids occurs at high stress value and low deformation rate.

The aim of this investigation was to simulate the influence of porous material heterogeneity in order to find out relation between the soft polymer material structure and its behaviour under the tension.

### EXPERIMENTAL

The finite element method (FEM) and method of photoelasticity (PEM) are used to derive simple formulae that relate Young's modulus and Poisson's ratio to porosity and microstructure of three different models. The displacements up to constant deformation  $\varepsilon = 0.2$  to the ends of the plane model were applied. The deformation scheme is presented in Fig. 1, a. The obtained models over-simplified representation of porous materials structure, which was observed in many natural or manufactured composite materials. Three types of plane models, which differ in porous size and its distribution mode, were investigated. Model I (Fig. 1, b) was designed only with one-sized pores. They lies in parallel rows with equal distance between pores in each direction. The diameter of these pores was  $d_1$ . Model II (Fig. 1, c) was created on the basis of Model I: symmetrically additional porous

\* Corresponding author. Tel.: +370-37-300205; fax: +370-37-353989. E-mail address: Daiva.Zeleniakiene@ktu.lt (D. Zeleniakienė)

elements, diameter of which was  $d_2 < d_1$  were added in interpores zones, founded between pores diameter of which was  $d_1$ . The Model III contains pores of three sizes, which were changed to according selected criteria:  $d_3 < d_2 < d_1$ . Schematically this model is presented in Fig. 1, d.

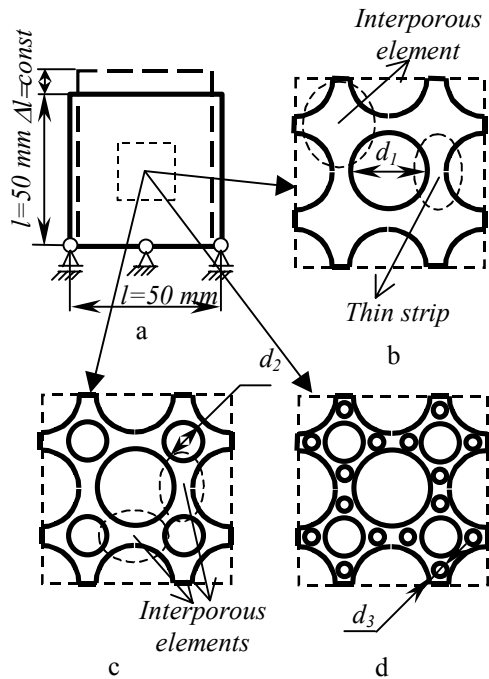


**Fig. 1.** The deformation scheme (a) and schematic view of Model I (b), Model II (c) and Model III (d)

In order to predict properties or properly to interpret relationship between the tensile behaviour and microstructure of porous material, the influence of main structural parameter such as material porosity for all types of models has been investigated. This parameter was evaluated according to changes of pores diameter  $d_1$ ,  $d_2$  and  $d_3$ . The ratio between pores diameter and length of model  $l$  was proportionally changed according these expressions:  $d_1/l = 0.01 \div 0.20$ ,  $d_2/l = 0.02 \div 0.12$ ,  $d_3/l = 0.02 \div 0.04$ . In all cases the distance between pores centres was constant.

For volume porous body porosity is defined as the ratio of the volume of voids to the total volume of body. Thus, for the plane body porosity  $\gamma_p$  can be determined from relation

$$\gamma_p = \frac{\sum_{i=1}^m S'_p}{S'_{mod}} = \frac{\pi(n_1^2 d_1^2 + n_2^2 d_2^2 + n_3^2 d_3^2)}{4l^2}, \quad (1)$$

where  $S'_p$ ,  $S'_{mod}$  are the square of model and pores, respectively;  $n_1$ ,  $n_2$ ,  $n_3$ , – the amount of pores in the row (the subnumbers relates to pores diameter  $d_1$ ,  $d_2$ ,  $d_3$ );  $l$  is the plane dimensions of model;  $m$  is the amount of pores types.

Assuming that dimensions of the plane model are equal to the cross-section dimensions of cubic model with gradually distributed spherical pores, the volume porosity  $\gamma_i$  can be expressed as

$$\gamma_i = \gamma_p \frac{2(n_1^3 d_1^3 + n_2^3 d_2^3 + n_3^3 d_3^3)}{3l(n_1^2 d_1^2 + n_2^2 d_2^2 + n_3^2 d_3^2)}. \quad (2)$$

The plots after solution of this equation for different porosity cases are presented in Fig. 2. Seems, that for all investigated porosity cases the curve mode depends on the distribution of main and additional pores in all models.

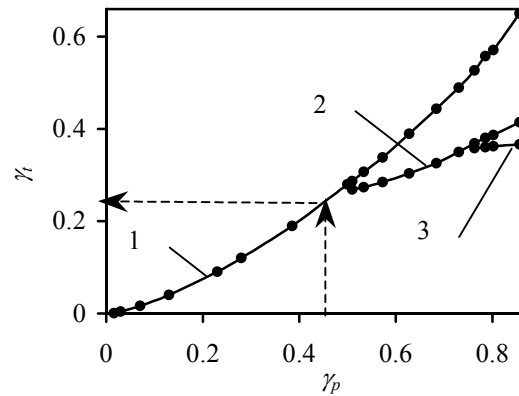


**Fig. 2.** The relation between plane  $\gamma_p$ , and volume  $\gamma_i$  porosity for Model I (1), Model II (2), Model III (3)

The method of photoelasticity and principals of non-linear theory of elasticity, adopted for high deformations and special mathematical treatment were used to investigate stresses and strain distribution in created models [11, 12].

The models for these investigations were prepared from optical sensitive urethane rubber SKU 10-4b Young's modulus of which was  $E = 3.98$  MPa and Poisson's rate was  $\mu = 0.46$ .

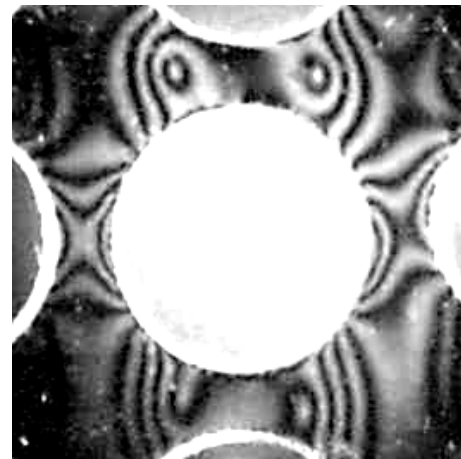


**Fig. 3.** The typical isochromatic view of the porous sample obtained by PEM for Model I

Evaluations were performed according to the obtained isochromatic fringe pattern (Fig. 3). The isochromes (dark lines) are the contours of equal principle stress difference  $\sigma_1 - \sigma_2$ . The relation between isochrome number and stress difference presents the main equation of photoelasticity known as Verhaim equation [13]

$$\delta = Ch_0 \lambda_3 (\sigma_1 - \sigma_2) \quad (3)$$

where  $\delta$  is the optical path length difference,  $C = 2.905 \times 10^{-6} \text{ m}^2/\text{kN}$  is optical constant,  $\sigma_1$  and  $\sigma_2$  are the principal stresses,  $h$  is the thickness of the specimen,  $\lambda_3$  is the principal elongation value in light source direction.

Analysis of local stresses by finite element method was conducted by commercial code ALGOR. The model was made utilised symmetry and periodicity, assuming that there are no stresses trough-the thickness in the plane. Four-node quadri-lateral "PLANE" elements with four degrees of freedom in each node were used. Exact number of elements of each model depends on the model type and porosity it represents. The both Young's modulus and Poisson's ratio are the same as used for photoelastic investigations.

## RESULTS AND DISCUSSIONS

The role of porosity on polymer material mechanical behaviour was evaluated according to the changes of principal stresses  $\sigma_1$  value. The changes were evaluated by means of stress concentration factor  $K_\sigma$ :

$$K_\sigma = \frac{\sigma_1}{\sigma_{1N}}, \quad (4)$$

where  $\sigma_1$  is the value of principal stress in control point,  $\sigma_{1N}$  is the nominal stress caused in nonporous material.

**Model I.** The influence of material porosity  $\gamma_p$  on stress concentration factor changes for Model I is presented in Fig. 4. Seems, that for low material porosity ( $\gamma_p = 0.002$ ) the stresses shows 3 times higher stress concentration values, than those in nonporous material, for which  $K_\sigma = 1$ .

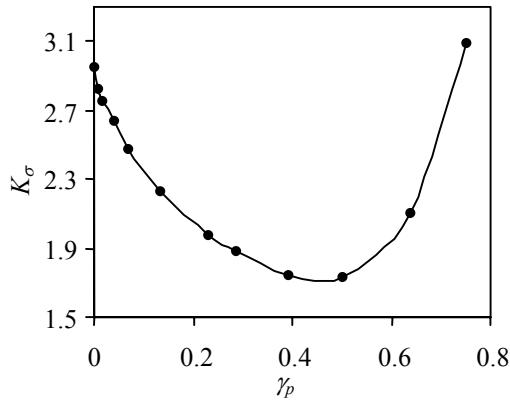


**Fig. 4.** The relationship of stress factor  $K_\sigma$  with respect to porosity  $\gamma_p$  for Model I

As the material porosity increases up to 0.5, the significant decrease of concentration factor values is obtained. In this case stresses decrease more than two fold compare with previous observed case. Otherwise, they are only 1.7 times higher than those of nonporous material. These results show that in the polymer rarely distributed small pores do not decrease material stiffness, but they act like small cracks in top of which high stressed regions appear and suitable conditions for failure initiation are created. Obviously, that the increase of pores diameter influence on the decrease of polymer quantity in the overall material. That results on the more even stress field distribution and elimination of high stressed zones.

The changes of stress concentration factor values suggest that porosity can be accepted as parameter, which influences on the material stiffness, proportionally to the relation

$$E_{pm} \approx E_{nm} \cdot \frac{S_{nm} - \sum S_p}{S_{nm}}, \quad (5)$$

where  $E_{pm}$  and  $E_{nm}$  is the Young's modulus of porous and pure polymer.  $S_{nm}$  and  $S_p$  are the area of cross section of porous and pure polymer, respectively.

So, the increase of material porosity (pores diameter) decreases porous material stiffness  $E_{pm}$ . That results on the decrease of deformation force  $F_{pm}$ , which is needed to apply in order to deform body up to deformation value  $\varepsilon$ . Deformation force  $F_{pm}$  which are also the external tensile force of material can be presented according to the following expression

$$F_{pm} = \sigma_{pm} \cdot S_{pm} = \sigma_{pm}(S_{nm} - \sum S_p), \quad (6)$$

there  $S_{pm}$  is the area of porous material cross sections. After embedding values of  $S_{nm}$  and  $S_p$  to (6),  $F_{pm}$  can be defined as

$$F_{pm} = \sigma_{pm} h(l - n_1 d_1), \quad (7)$$

Assuming that for Model I the values of pores diameter  $d_2$  and  $d_3$  are equal to zero, from (1) follows

$$d_1 = \frac{2l}{n_1} \cdot \sqrt{\frac{\gamma_p}{\pi}}, \quad (8)$$

then (7) can be written as

$$F_{pm} = \sigma_{pm} h l \left( 1 - 2 \sqrt{\frac{\gamma_p}{\pi}} \right). \quad (9)$$

The nominal tensile force  $F_N$  of pure material is equal to

$$F_N = \sigma_{nm} \cdot S_{nm} = \sigma_{pm} \cdot (S_{nm} - \sum S_p) = \sigma_{pm} \cdot S_{nm} = \sigma_{pm} h l. \quad (10)$$

If (9) and (10) will be presented as ratio, the following relation can be written

$$\frac{F_{pm}}{F_N} = 1 - 2 \sqrt{\frac{\gamma_p}{\pi}} = 1 - 1.28 \sqrt{\gamma_p}. \quad (11)$$

So, from (11) it is clear seen that the increase of material porosity leads to the decrease of relative deformation force. The theoretical results obtained according to these calculations and those by methods of FEM and PEM are presented in Fig. 5. In all cases the relative difference between obtained results was not higher than 8 %.

As the porosity is higher than  $\gamma_p = 0.5$ , independently on the decrease of relative deformation force, stresses monotonously increases (Fig. 4). For this porosity mode ( $\gamma_p > 0.5$ ) significant changes of material geometry appear. Between pores in equator zones only thin material tapes are formed, but interpores zones are relatively large and wide (Fig. 1, b). Due to high geometry changes the stresses markedly increase and in the case of porosity equal to  $\gamma_p = 0.75$ , they are 3.1 times higher than those in pure material.

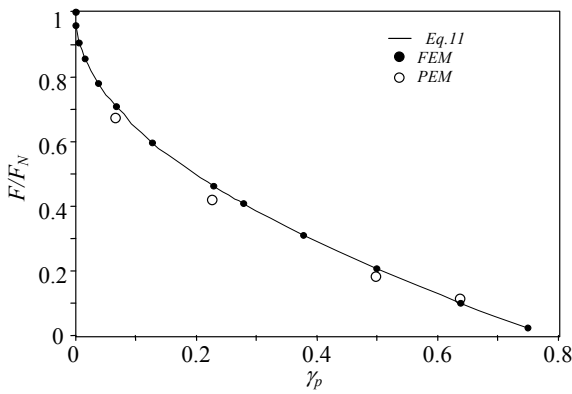


**Fig. 5.** The changes of relative force  $F_{pm}/F_N$  in dependence of porosity  $\gamma_p$  for Model I

**Model II.** The Model II contains pores diameter of which was  $d_1$  and  $d_2$  (Fig. 1, c). The model was created in such way that the diameter of pores  $d_1$  will be equal to those, in which lowest stress concentration for Model I was found. They were equal to  $0.16l$ . The material porosity was changed only by variation in pores diameter  $d_2$ . Location of them was found in the interpores zones created between pores  $d_1$ . The influence of material porosity on the stress state changes was evaluated according to the obtained stress values in selected control points. Its location are presented in Fig. 6, a.

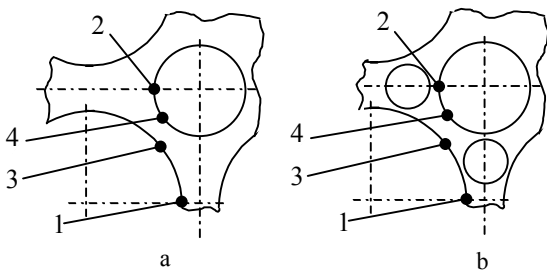


**Fig. 6.** The location of control points for stress state evaluation in porous Model II (a) and Model III (b)

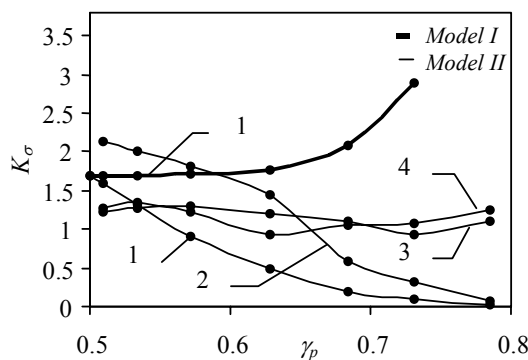


**Fig. 7.** The changes of stress concentration factor  $K_\sigma$  in dependence on material porosity  $\gamma_p$  for Models I and Models II (curves numbered according to Fig. 6, a)

The results of these investigations are plotted in Fig. 7. Seems, that independently on control point location the stress concentration factor values in all investigated porosity cases for Model II is lower than that for Model I. The exception is control point 2, for which up to material

porosity  $\gamma_p=0.6$  stresses are higher than those for Model I. As the material porosity increases redistribution of stresses appear and maximum stress values are obtained not in the points zones 1 and 2, but in those of points 3 and 4. On the other hand, the changes of the material porosity practically do not influence stress values in control points 3 and 4. In that time for control points 1 and 2 the significant decrease of stress values with the increase of material porosity is characteristic. For this model the lowest stress values were obtained at material porosity  $\gamma_p=0.73$ , but they are 20 % higher than those of pure material.

The geometrical structure of **Model III** was created on the base of Model II. There, the additional pores, diameter of which was  $d_3$  in the interpores zone were added (Fig. 1, d, and Fig. 6, b). The porosity was changed only varying in pores  $d_3$  diameter. Pores diameter  $d_1$  and  $d_2$  was constant. It values were chosen in that way in which stress concentration for Model II was lowest, i.e. those for porosity  $\gamma_p=0.73$ .

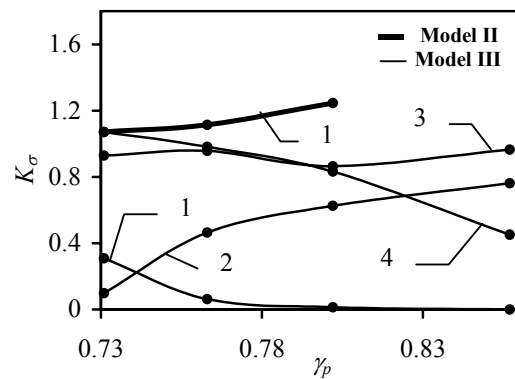


**Fig. 8.** The influence of material porosity  $\gamma_p$  on stress concentration factor  $K_\sigma$  changes for Model II and Model III (numbered according to Fig. 6, b)

The obtained results are presented in Fig. 7. Seems, that the mode of stress changes depends not only on the size of material porosity, but on the control point location, also. For this porosity mode non-monotonous stress distribution is characteristic. The decrease of stress values in control points 1 and 4 and the significant increase of them in control point 2 with the increase of material porosity was observed. Otherwise, the porosity changes practically do not influence the stress state in the zone of point 3. There only negligible changes of stress values were found and in all cases they are very close to those of nonporous material. In that time the stress concentration factor values in the control points 1, 2 and 4 suggest that stress values are lower than in nonporous material, because  $K_\sigma < 1$ .

**The influence of pores shifting.** As a rule in the volume of real polymer body pores are distributed irregularly. In order to find out relation between porous distribution irregularities (mode) and stress state the investigation on the basis of Model I was carried out. The porosity mode changes were realized by every other pores row shifting by step  $\Delta$  in rows direction. The stress field changes after this kind of transformations are presented in Fig. 9.

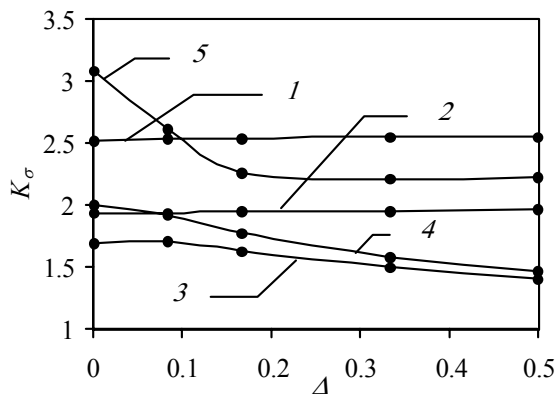


**Fig. 9.** The influence of size of shifting step  $\Delta$  on stress concentration factor  $K_\sigma$  for Model I for different porosity cases: 1- 0.03; 2 – 0.23; 3 – 0.5; 4 – 0.64; 5 – 0.75

Seems, that more markedly stress field changes was observed only for models which porosity is higher than 0.5, i.e. which simulate composition with both the low distance between pores and small interpores zones. Besides, the influence of pores shifting is higher the higher porosity value. This effect can be explained by the fact that the increase of shifting step  $\Delta$  and increase of material porosity eliminate stiff interpore zones. Due to this drastic changes of material geometry disappear, stress distribution becomes more even and the stress concentration decreases.

## CONCLUSIONS

The experimental photoelasticity and numerical finite element methods were used for the identification the stress state in soft polymer material in dependence on porous size and its distribution mode.

Application of these methods showed that the highest local stress values are created in the polymer and pore boundary zone. Both the porosity size and its distribution mode influence the stress values. It was obtained that the appearance of small and rare pores results in creation of high stressed local regions in the interface. They act as defects of polymer and can be accepted as zones of failure initiation. Besides, evenly distributed same diameter pores results on the increase of stress values in boundary layer, also.

The high material porosity and the absence of large interpores zones cause only insignificant stress concentration values. In some cases obtained values can be lower than those in nonporous material.

The irregularities of pores distribution mode influence the stress state only in the case of high material porosity ( $\gamma_p > 0.5$ ).

## REFERENCES

1. **Roberts, A. P., Knackstedt, M. A.** Structure – Property Correlations in Model Composite Materials *Physical Review E* 54 1996: pp. 2313 – 2328.
2. **Savin, G. N.** Investigation of Stress Near Hole. Kiev, Naukova Dumka, 1968: 887 p. (in Russian).
3. **Royle, D.** Mechanics of Materials. New York, John Wiley & Sons Inc, 1996: 315 p.
4. **Anderson, T. L.** Fracture Mechanics: Fundamentals and Applications. CRC Press, 1991: 793 p.
5. **Hertzberg, R. V., Manson, J. A.** Fatigue of Engineering Plastic. Academic Press, 1980: 292 p.
6. **Lu, G., Lu (Max), G. Q., Xiao, Z. M.** Mechanical Properties of Porous Materials *Journal of Porous Materials* 6 (4) 1999: pp. 359 – 368.
7. **Roberts, A. P., Garboczi, E. J.** Elastic Properties of Model Porous Ceramics *Journal of the American Ceramic Society* 83 (12) 2000: pp. 3041 – 3058.
8. **Roberts, A. P., Garboczi, E. J.** Elastic Moduli of Model Random Three – Dimensional Closed – Cell Cellular Solids *Acta Materialia* 49 (2) 2001: pp. 189 – 197.
9. **Andrews, E. W., Gibson L. J.** The Influence of Crack – Like Defects on the Tensile Strength of an Open – Cell Aluminium Foam *Scripta Materialia* 44 (7) 2001: pp. 1005 – 1010.
10. Handbook of Technical Textiles, ed. **Horrocks, A. R., Anand,** CRC Press, 2000: 559 p.
11. **Froxt, M.** Photoelasticity. Moscow, State Publish House of Technic, Theoretical Literature, Vol. 1, 1948: 432 p. (in Russian).
12. **Froxt, M.** Photoelasticity. Moscow, State Publish House of Technic, Theoretical Literature, Vol. 2, 1950: 488 p. (in Russian).
13. **Liukaitis, J.** Investigation of Stress and Strain in Soft Polymeric Material Constructions. Kaunas, Technologija, 1994: 184 p. (in Lithuanian).

DOI: 10.5755/j02.ms.26705